Cyclic Extrusion of Poly(butylene terephthalate)/ Organo-Montmorillonite Nanocomposites: Thermal and Mechanical Retention Properties

Wen Shyang Chow

School of Materials and Mineral Resources Engineering, Engineering Campus, Universiti Sains Malaysia, 14300 Penang, Malaysia

Received 7 December 2006; accepted 14 May 2008
DOI 10.1002/app.28804
Published online 25 July 2008 in Wiley InterScience (www.interscience.wiley.com).

ABSTRACT: Poly(butylene terephthalate) (PBT) containing 3 wt % of organo-montmorillonite (OMMT) was prepared using twin screw extrusion followed by injection molding. The effects of thermal cycles (two times extrusion followed by injection molding) were studied on both PBT and PBT/OMMT nanocomposites. The samples were characterized by using tensile tests, flexural tests, field-emission scanning electron microscopy (FESEM), X-ray diffraction (XRD), differential scanning calorimetry (DSC), thermogravimetry analysis (TGA), and dynamic mechanical thermal analysis (DMTA). The intercalation of the OMMT silicate layers in the PBT was confirmed using XRD. Both tensile and flexural modulus of PBT was improved by addition of OMMT. DSC results revealed that OMMT improved the crystallinity of PBT. The percentage retention in tensile and flexural properties of PBT/OMMT(E2) intercalated nanocomposites (i.e. two times extrusion followed by injection molding) is more than 96%. The melting temperature, crystallization temperature, and degree of crystallinity of PBT/OMMT(E2) is comparable with PBT/OMMT(E1) (i.e. one time extrusion followed by injection molding). This indicates that PBT/OMMT intercalated nanocomposites exhibit good retention-ability in mechanical and thermal properties after subjecting to two times twin-screw extrusion followed by injection molding. From the TGA results, it was observed that the thermal stability (e.g. T_{onset}) of PBT was reduced by the addition of OMMT. However, the addition of OMMT assists in the char formation of PBT. © 2008 Wiley Periodicals, Inc. J Appl Polym Sci 110: 1642–1648, 2008

Key words: poly(butylene terephthalate); organoclay; nanocomposites; extrusion; thermal properties

INTRODUCTION

Polymer nanocomposites have received considerable attention and great interest in industry and academia. The addition of nanometer scale reinforcement may dramatically improve selected properties of the related polymer. These nanocomposites exhibit superior properties such as enhanced mechanical properties, reduced permeability, and improved flame retardancy.[1] Polymer layered-silicate nanocomposites are currently prepared in four ways: *in-situ* polymerization, solution intercalation, direct melt intercalation, and sol–gel technology. Direct polymer melt intercalation is the most attractive way because of its low cost, high productivity, and compatibility with current processing techniques.[2] Naturally occurring montmorillonite is the most abundant member of the smectite family of clays. However, naturally occurring montmorillonite is incompatible with most polymers because of its hydrophilic nature. Ion exchange is widely practiced to modify the montmorillonite's surface to increase its compatibility with mostly hydrophobic polymers. Thus, the using of organo-montmorillonite (OMMT) could enhance its compatibility with organic polymers.[3]

PBT resins are semicrystalline thermoplastics used in a wide variety of applications, most commonly in durable goods that are formed by injection molding.[4] Several researchers had described polymer-clay nanocomposites based on PBT.[5–9] PBT/organoclay nanocomposites have been prepared by *in situ* interlayer polymerization, in which the clay layer was found to be highly dispersed on a nanometer scale. The thermo-mechanical properties of the PBT were improved by the addition of small amount of organoclay.[5] Direct melt intercalation methods have been used to prepare PBT/organoclay and PBT/cetyl pyridium chloride modified montmorillonite nanocomposites.[6,7] The formation of exfoliated-intercalated structure of the PBT/clay nanocomposites has

Correspondence to: W. S. Chow (shyang@eng.usm.my).
Contract grant sponsor: Malaysia Toray Science Foundation (MTSF) Science and Technology Research Grant 2005.

been confirmed by X-ray diffraction and transmission electron microscopy (TEM) analysis. The melting temperature, crystallization rate, and crystallinity of the PBT were improved by the incorporation of modified montmorillonite.[7] Li et al.[6] have investigated the modification of MMT by three different alkylammonium surfactants and studied the intercalation/exfoliation behavior of PBT nanocomposites. Acierno et al.[8] have studied the relationships between processing conditions, hybrid composition, nanoscale morphology, and properties of PBT nanocomposites based upon several commercial OMMT at different weight percentages. Chang et al.[9] have studied the melt intercalation of PBT/OMMT nanocomposites by using twin screw extrusion. The nanocomposites based on the higher-viscosity PBT showed a higher degree of exfoliation of the clay and a higher reinforcing effect when compared with the composites based on the lower-viscosity PBT.

In the previous work, it was found that the optimum loading of OMMT in PBT is attained at 3 wt %. Thus, in the present work, 3 wt % of OMMT was selected and the PBT/organo-montmorillonite (OMMT) nanocomposites were prepared by direct melt intercalation method. The samples were produced by twin screw extrusion followed by injection molding. The present work has been devoted to study the effects of OMMT on the mechanical and thermal properties of PBT/OMMT nanocomposites. The effects of thermal cycles (two times extrusion followed by injection molding) were also studied on both PBT and PBT/OMMT nanocomposites. Repeated extrusion could be related to the recycling processes. The present work also attempted to study the recycleability of the PBT/OMMT nanocomposites.

MATERIALS AND EXPERIMENTAL

Materials

The poly(butylene terephthlate) (PBT^{TM}, Toraycon) was supplied by Toray, Japan. Octadecyl amine treated montmorillonites (Nanomer 1.30E-OMMT) was supplied from Nanocor, USA. In this work, 3 wt % of OMMT was incorporated into PBT. The samples were labeled as PBT(E1), PBT/OMMT(E1), PBT(E2), and PBT/OMMT(E2).

Preparation of PBT/OMMT nanocomposites

Melt compounding of the PBT and PBT/OMMT nanocomposites was done on a counter-rotating twin-screw extruder (Berstoff). The extrusion temperature zone ranged from 220 to 240°C. Before extrusion, PBT pellets and OMMT were dehumidified by using a vacuum oven at 80°C for 8 h. The extrudates were pelletized with a Haake pelletizer. For PBT(E1) and PBT/OMMT(E1) nanocomposites, the samples were prepared by one time extrusion followed by injection molding. However, for PBT(E2) and PBT/OMMT(E2) nanocomposites, the samples were prepared by two times extrusion processes followed by injection molding.

Characterization of PBT/OMMT nanocomposites

Tensile tests were performed on an Instron-3366 machine at 23°C, according to ASTM D638, at a crosshead speed of 50 mm/min. The tensile modulus, tensile strength, and elongation at break were evaluated from the stress–strain data. Flexural testing of the PBT composites was performed according to ASTM D790, with an Instron 3366 machine equipped with three-point bending rig. The testing speed was set at 100 and 150 mm/min. The percentage retention of the tensile and flexural properties was calculated.

The morphology of the PBT and PBT/OMMT specimens was inspected in a field-emission scanning electron microscopy (FESEM, Zeiss Supra 35VP). The samples were gold coated to avoid electrostatic charging during examination. Wide-angle X-ray spectra were recorded with a D5000 diffractometer (Siemens, Germany) in step scan mode using Ni-filtered Cu K_α radiation (0.1542 nm wavelength). Powder samples were scanned in reflection, whereas the injection-molded compounds were scanned in transmission in the interval of $2\theta = 1^\circ - 10^\circ$. The interlayer spacing of the OMMT was derived from the peak position (d_{001}-reflection) in the XRD diffractograms according to the Bragg's equation ($\lambda = 2\ d \sin\theta$).

The melting and crystallization behavior of the PBT and PBT/OMMT nanocomposites were studied under nitrogen atmosphere by differential scanning calorimetry (Perkin Elmer DSC-6), using 8–10 mg sample sealed into aluminum pans. The temperature was raised from 30–260°C at a heating rate of 10°C min^{-1}, and after a period of 1 min, it was swept back at −10°C min^{-1}. Second heating similar to the first heating was then performed. Thermogravimetry analysis (TGA) was carried out on a Perkin Elmer Pyris 6 thermogravimetric analyzer (USA). The sample weight for TGA tests is ~ 20 mg. The PBT and PBT/OMMT nanocomposites were heated from room temperature to 580°C at a heating rate of 20°C/min under nitrogen atmosphere.

Dynamic mechanical thermal analysis (DMTA) test was conducted according to ASTM D5023. The storage modulus (E'), loss modulus, and mechanical loss factor ($\tan\delta = E''/E'$) as a function of temperature (T), were assessed by using a Mettler Toledo DMA 861, Switzerland. DMTA spectra were taken in

3-point bending mode at 1 Hz frequency in a temperature ranged from −30 to 180°C.

RESULTS AND DISCUSSION

XRD analysis of PBT/OMMT nanocomposites

In XRD patterns the interlayer spacing of clay can be determined by the site of the peak corresponding to the {001} basal reflection of MMT (referred to as d_{001} peak).[10] Figure 1 shows the XRD patterns in the range of $2\theta = 1 - 10^\circ$ for OMMT, PBT/OMMT(E1), and PBT/OMMT(E2). The XRD spectrum of OMMT exhibits a broad intense peak at around $2\theta = 4.35^\circ$ corresponding to a basal spacing of 2.03 nm. The XRD spectra of both PBT/OMMT(E1) and PBT/OMMT(E2) show a new peak at around $2\theta = 2.85^\circ$ corresponding to a basal spacing of 3.10 nm. Note that the d_{001} peaks in PBT/OMMT nanocomposites are shifted to a lower angle. This indicates that PBT chains diffuse into the gallery of the OMMT and the interspacing of silicate layers in OMMT is swollen to a larger distance. This is likely to reflect that the OMMT has been successfully intercalated into the PBT matrix. For intercalated nanocomposites, the finite layer expansion associated with the polymer intercalation results in the appearance of a new basal reflection corresponding to the larger gallery height (interlayer spacing).[1] The XRD patterns of PBT/cetyl pyridium chloride modified montmorillonite (OMT-CPC) showed a broadened peak around 3.27 nm, however, the average basal spacing of the OMT-CPC is 2.38 nm. The increment of the basal spacing indicates that the clay layers are partially intercalated and partially exfoliated in the PBT matrix.[7] The increase in interlayer distance of PBT/organic montmorillonite (MMT 10 A) indicates the formation of intercalated nanocomposites.[10] From Figure 1, it can be seen that two peaks at $2\theta = 2.7$ and 2.85 were observed for the PBT/OMMT(E1). However, it seems like only one peak at $2\theta = 2.85$ is observed for PBT/OMMT(E2). Recall that PBT/OMMT(E2) nanocomposites have been subjected to two-times extrusion processes. It is believed that some of the amount of organic intercalant (octadecylamine) might decompose after subjected to repeated extrusion processes. Subsequently, some of the interlayer spacing of OMMT might be collapsed and slightly reduce the *d*-spacing of OMMT.

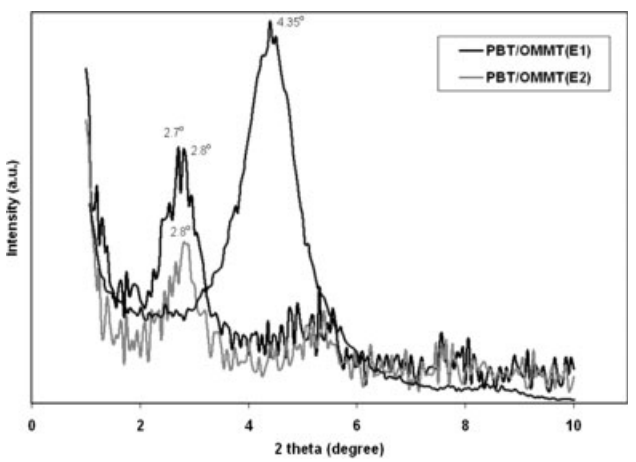

Figure 1 XRD spectra of OMMT and PBT/OMMT nanocomposites.

Mechanical properties of PBT/OMMT nanocomposites

Figure 2(a–d) shows the effects of OMMT on the tensile properties of PBT. The tensile modulus of PBT increased with the addition of OMMT. This is attributed to the stiffness and reinforcing effects of OMMT. The OMMT is able to act as reinforcing filler due to its high aspect ratio and platelet structure. The possibility that the modulus improvements are due to the constraint of the polymer chains by the interaction with the clay surface.[11] Note that the tensile strength of PBT/OMMT nanocomposites is higher than that of unfilled PBT. This is believed to be associated to the interfacial interaction between the PBT and OMMT. The elongation at break of PBT decreased in the presence of OMMT. This is likely due to the co-existence of agglomerated layered silicates, and intercalated OMMT silicate layers in the PBT matrix. It is interesting to note that the percentage retention of the tensile properties of PBT/OMMT after subjected to thermal cycle (i.e. two times extrusion followed by injection molding) is more than 96% for tensile modulus, strength, and elongation at break.

Table I shows the flexural modulus and strength of PBT and PBT/OMMT nanocomposites. The flexural tests were carried out at two different speeds, i.e. 100 and 150 mm/min. It can be seen that the flexural modulus of PBT was increased by the addition of OMMT. This is due to the intercalation and reinforcing effects of OMMT. The two different testing speeds did not have much influence on the flexural properties of PBT and PBT/OMMT nanocomposites. The percentage of retention for flexural modulus and strength of PBT/OMMT nanocomposites (PBT/OMMT(E2)) was higher than 98% as the testing speed is 100 mm/min.

Morphological properties of PBT/OMMT nanocomposites

Figure 3(a,b) shows the FESEM micrographs taken from the tensile fractured surface of PBT/OMMT(E1) and PBT/OMMT(E2), respectively. Fibrillated morphology

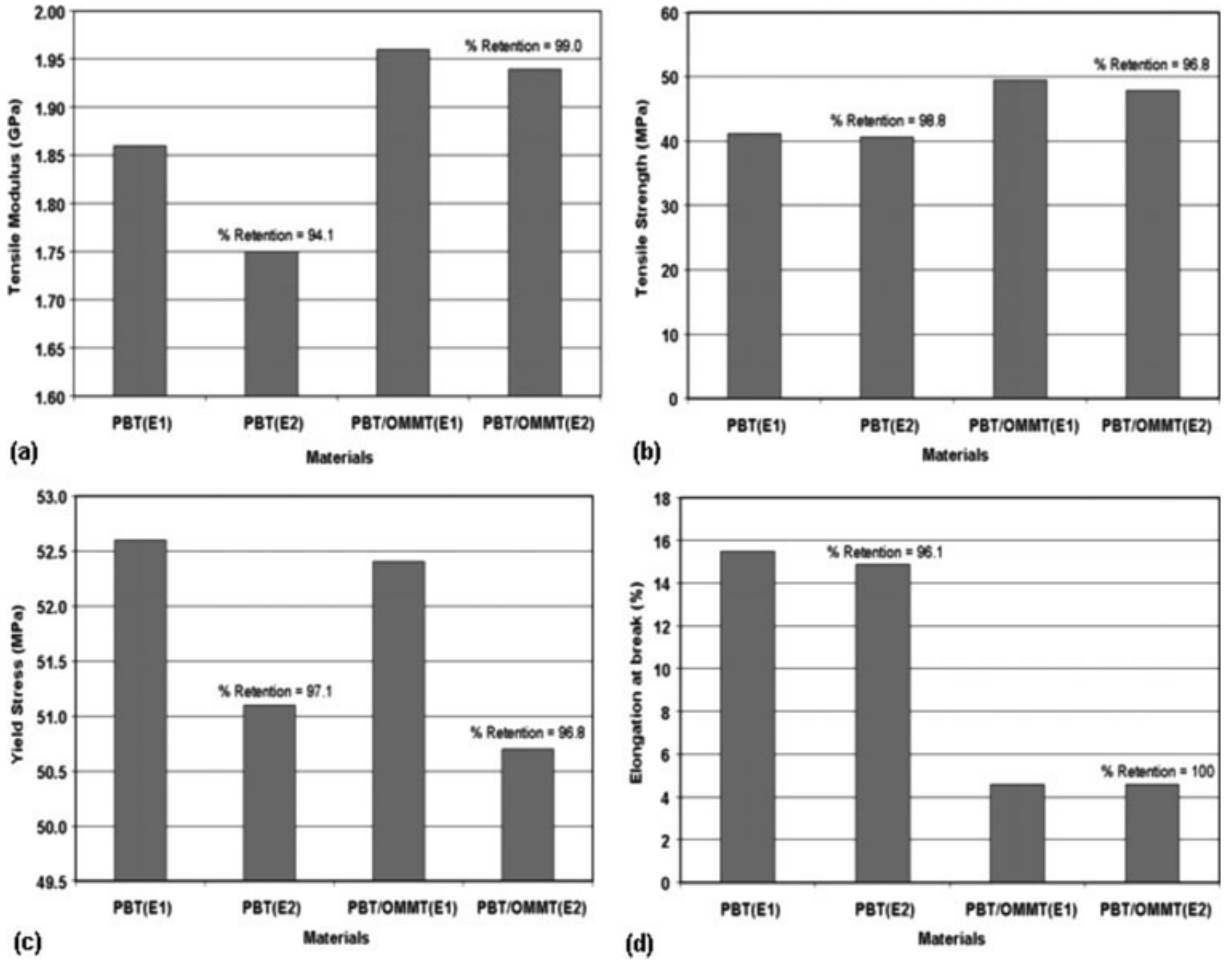

Figure 2 (a) Tensile modulus of PBT and PBT/OMMT nanocomposites (b) Tensile strength of PBT and PBT/OMMT nanocomposites (c) Yield stress of PBT and PBT/OMMT nanocomposites (d) Elongation of break for PBT and PBT/OMMT nanocomposites.

was observed for both PBT/OMMT(E1) and PBT/OMMT(E2). From Figure 3(a), it can be seen that particles adhere with PBT fibrillated structure (shown by arrow). The particle size is $\sim$ 6 μm. This indicates that some of the OMMT particles remain unexfoliated. From Figure 3(b), it can be revealed that some small particles (shown by arrow) dispersed in the PBT matrix. The particles are in the range of 2 μm. This may suggest that the two-time extrusion might facilitate the de-agglomeration of OMMT into a relatively smaller size.

Thermal properties of PBT/OMMT nanocomposites

Figure 4(a,b) show the DSC thermograms of PBT samples recorded from the first heating and second heating, respectively. The endothermic peak of pure PBT

TABLE I
Flexural Properties of PBT and PBT/OMMT Nanocomposites

Flexural properties	PBT(E1)	PBT(E2)	PBT/ OMMT(E1)	PBT/ OMMT(E2)
Testing speed = 100 (mm/min)				
Flexural modulus (GPa)	2.47	2.47 (100.0%)	2.51	2.49 (99.2%)
Flexural strength (MPa)	98.1	97.0 (98.9%)	94.6	92.7 (98.0%)
Testing speed = 150 (mm/min)				
Flexural modulus (GPa)	2.47	2.51 (101.6%)	2.50	2.45 (98.0%)
Flexural strength (MPa)	99.5	100.5 (101.0%)	98.3	95.1 (96.7%)

The values in the parentheses are the percentage retention of the flexural properties after thermal cycles (2 times extrusion followed by injection molding).

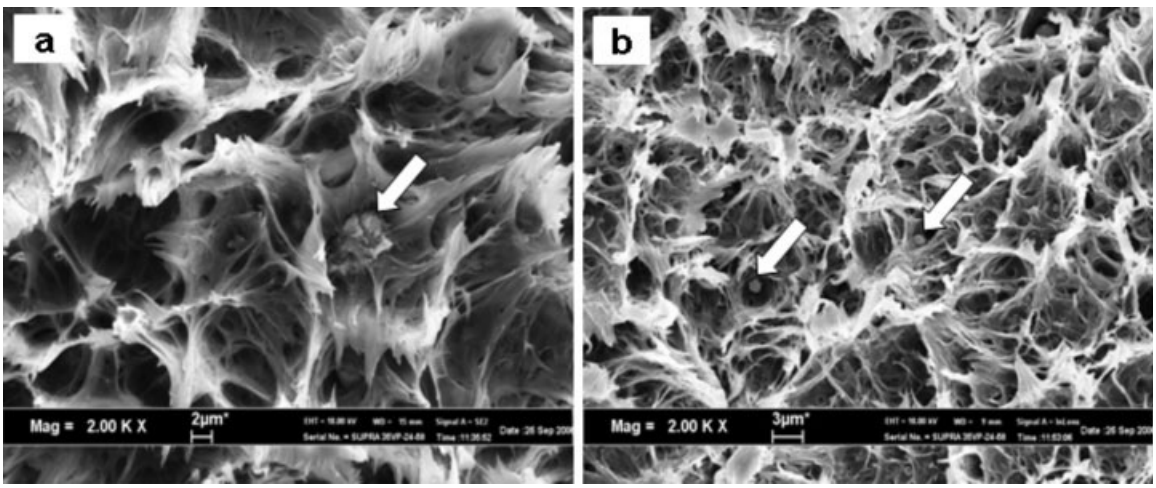

Figure 3 (a) FESEM taken from the tensile fractured surface of PBT/OMMT(E1) (b) FESEM taken from the tensile fractured surface of PBT/OMMT(E2).

appears at 227°C and corresponding to the melting temperature (T_m). Note that only one melting endothermic peak is observed from the first heating. However, two melting endothermic peaks are recorded during second heating for both PBT and PBT/OMMT nanocomposites. The double melting endotherm could be attributed to the presence of morphologically different crystal structures, for example, the existence of folded chain crystals containing partially extended chains. Multiple melting endothermic peaks could be revealed as a result of the melting–recrystallization process during heating.[7] In a number of semicrystalline polymers, multiple peaks can be observed during a DSC scan when imperfect crystals that have melted at lower temperature, recrystallize to give crystals at a higher temperature. A second lower temperature melting endotherm in PBT arises attributed to the crystal growth in the amorphous phase and a corresponding reorganization in the higher-melting crystal structures. PBT may display double melting endotherms, especially when the samples have been slowly cooled from the melt. The two peaks reflect the formation of two distinct crystal types.[12] Double melting was observed in neat PBT and interpreted in terms of reorganization processes occurring during the second heating.[13] The occurrence of the small peaks, which appear as shoulders at slightly lower temperatures, may be because of the changes of crystal structure of PBT, changes in the crystallite size or perfection, or variation of crystal thickness.[14] Addition of OMMT did not alter the T_m and T_c of PBT significantly. The degree of crystallinity (χ_c) was calculated from the melting enthalpy ΔH_m (J/g) with $\Delta H_f = 140$ J/g (the theoretical value of enthalpy for 100% crystalline PBT homo-polymer).[13]

Table II shows the heat of fusion (H_m) and degree of crystallinity (χ_c) of PBT and PBT/OMMT nanocomposites. It is interesting to note that the degree of crystallinity of PBT increased in the presence of OMMT. This is attributed to the nucleation effects of OMMT and the improvement in the crystal perfection of PBT. A similar observation is reported by Mohd Ishak et al.[14] for the injection molded short

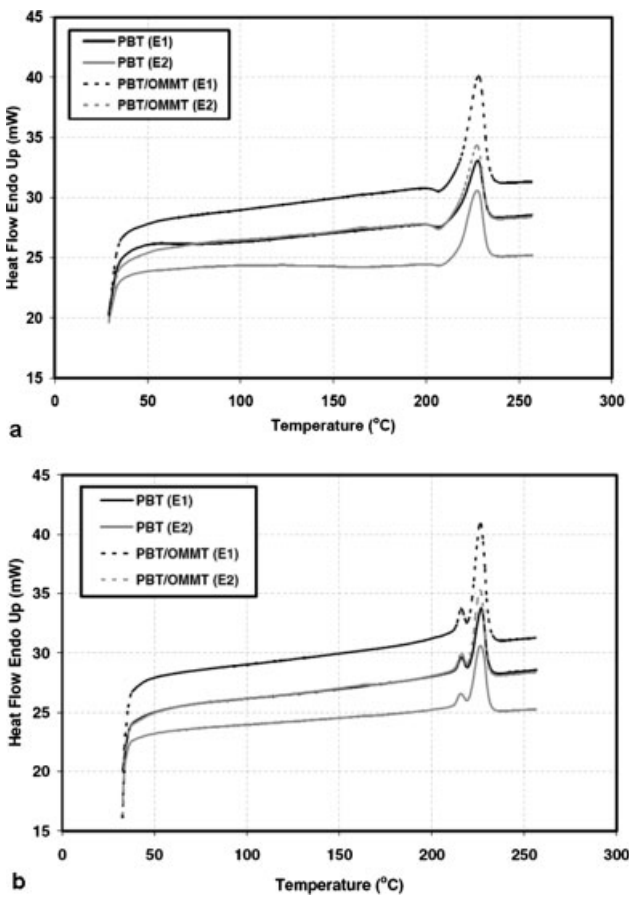

Figure 4 (a) DSC thermograms of PBT samples recorded from first heating (b) DSC thermograms of PBT samples recorded from second heating.

TABLE II
Degree of Crystallinity of PBT and PBT/OMMT Nanocomposites

	Thermal properties	
	H_m(J/g)	χ_c(%)
PBT(E1)	21.7	15.5
PBT(E2)	22.3	15.9
PBT/OMMT(E1)	29.2	21.7
PBT/OMMT(E2)	29.9	22.2

glass fiber reinforced PBT composites. From the thermal properties shown in Figure 4(b) and Table II, it can be seen that the T_m, T_c, and χ_c of PBT(E2) and PBT/OMMT(E2) which were subjected to thermal cycle (i.e. two times extrusion followed by injection molding) is essentially the same as that of PBT(E1) and PBT/OMMT(E1) (i.e.one time extrusion followed by injection molding). This suggests that the extra one time extrusion thermal cycles did not produce any apparent effect on the thermal behavior of PBT and PBT/OMMT nanocomposites.

Figure 5(a) shows the TGA curves of PBT and PBT/OMMT nanocomposites. Figure 5(b) shows the derivative weight-temperature curves of PBT and PBT/OMMT nanocomposites. It can be seen that the T_{onset} of PBT/OMMT is lower than that of PBT. The T_{onset} of PBT(E1) and PBT(E2) is $\sim$ 380°C, however, the T_{onset} of PBT/OMMT(E1) and PBT/OMMT(E2) is $\sim$ 345°C. This may be associated with the decomposition of the organic intercalant (octadecylamine) of OMMT and subsequently accelerates the decomposition of PBT. The clay may act as deformation accelerator at higher temperatures.[15] In the early stage of thermal decomposition, the clay would shift the decomposition to higher temperature. After that, this heat barrier effect would result a reverse thermal stability. The stacked silicate layers could hold accumulated heat that could be used as a heat source to accelerate the decomposition process.[1] From Figure 5(a), it can be seen that the char yield of PBT/OMMT is higher than that of pure PBT. This suggests that the addition of clay could assists in the formation of char after thermal decomposition.

The dynamic storage modulus and loss modulus versus temperature traces for the PBT and PBT/OMMT nanocomposites is shown in Figure 6(a,b),

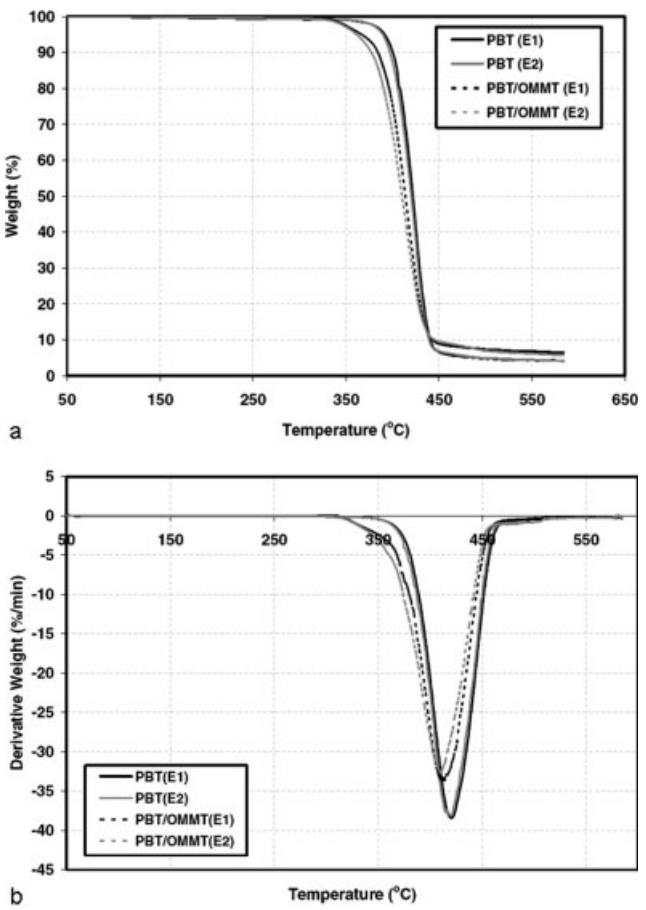

Figure 5 (a) TGA curves of PBT and PBT/OMMT nanocomposites (b) Derivative weight-temperature curves of PBT and PBT/OMMT nanocomposites.

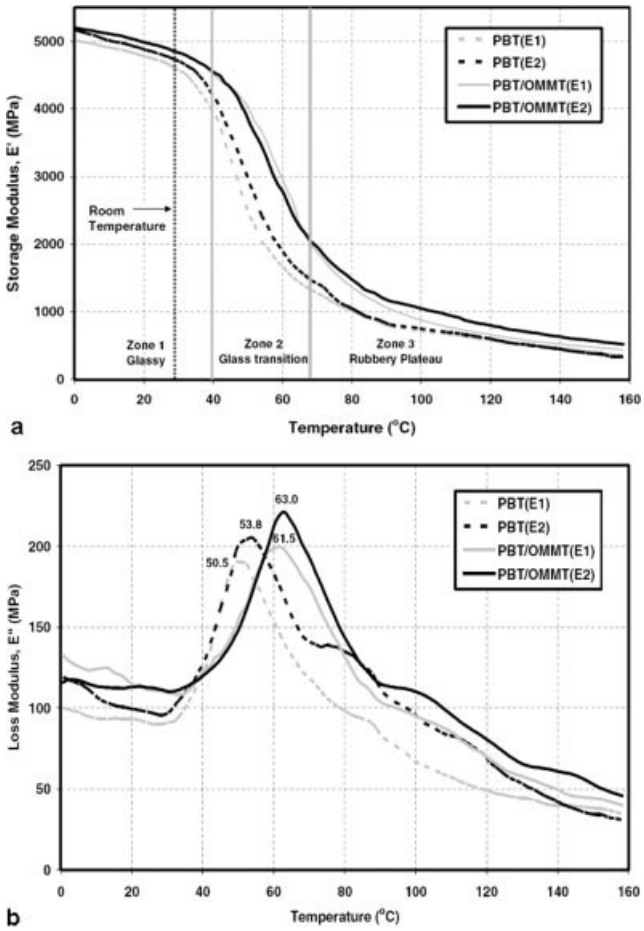

Figure 6 (a) Storage modulus versus temperature traces for PBT and PBT nanocomposites (b) Loss modulus versus temperature traces for PBT and PBT nanocomposites.

respectively. It can be seen that PBT/OMMT nanocomposites exhibit higher storage modulus than PBT [c.f. Fig. 6(a)]. The storage modulus of PBT(E2) is relatively higher than that of PBT(E1) in the whole temperature range. This may be attributed to the increasing crystallization and molecular arrangement of PBT after subjected to second time of extrusion. For the PBT/OMMT nanocomposites, the storage modulus of PBT/OMMT(E1) and PBT/OMMT(E2) was likely influenced by temperature zone. In the glassy zone (below 40°C), the storage modulus of both PBT/OMMT(E1) and PBT/OMMT(E2) is almost the same. In the glass transition zone (40 − 65°C), the storage modulus of PBT/OMMT(E1) was slightly higher than that of PBT/OMMT(E2). At the temperature more than 65°C, it can be seen that the storage modulus of PBT/OMMT(E2) is relatively higher compared to PBT/OMMT(E1). At room temperature, it can be seen that the storage modulus of PBT/OMMT is higher than that of PBT; this is in harmony with the tensile modulus [c.f. Fig. 2(a)]. In addition, the storage modulus of PBT/OMMT(E2) is comparable to PBT/OMMT(E1) nanocomposites.

Figure 6(b) shows the loss modulus versus temperature traces for the PBT and PBT/OMMT nanocomposites. Dynamic relaxation peak of PBT(E1) and PBT(E2) was recorded at 50.5 and 53.8°C, respectively. On the other hand, the dynamic relaxation peaks for PBT/OMMT(E1) and PBT/OMMT(E2) are 61.5 and 63.0°C, respectively. Note that the dynamic relaxation peaks of PBT/OMMT nanocomposites are higher than that of unfilled PBT. This may be attributed to the confinement of the intercalated polymer chains within the silicate clay galleries which could prevent segmental motions of the polymer chains. It is speculated that more chain confinement could occur when the PBT/OMMT is subjected to two-time extrusion processes. It is also believed that repeated extrusion processes could further increase the crystallizability of PBT/OMMT nanocomposites. One may observe that the dynamic relation peak of PBT and PBT/OMMT nanocomposites could be correlated with their degree of crystallinity (c.f. Table II). It can be seen that the degree of crystallinity of PBT/OMMT nanocomposites is higher than that of pure PBT. The trend of dynamic relation peak of PBT and PBT/OMMT nanocomposites are in harmony with their degree of crystallinity data obtained from DSC. Recall that the glass transition and dynamic relaxation peaks could be governed by several factors, e.g. chain mobility, chain flexibility, molecular weight, crystallinity, cross-linking density, and etc.

CONCLUSIONS

On the basis of this work devoted to study the effect of repeated extrusion on the thermal and mechanical properties of PBT/OMMT nanocomposites, the following conclusions can be drawn:

The OMMT has been successfully intercalated into PBT matrix. The thermo-mechanical properties of PBT were affected by the addition of OMMT. Modulus and strength of PBT were improved and attributed to the reinforcing effects and intercalationability of OMMT. The excellent percentage retention of both tensile and flexural properties of PBT/OMMT intercalated nanocomposites subjected to repeated extrusion processes suggested that the high recycleability of PBT/OMMT nanocomposites. The percentage retention in tensile and flexural properties of PBT/OMMT(E2) nanocomposites is more than 96%. The thermal properties of PBT/OMMT nanocomposites were governed by the range of temperature, which is evidenced by DSC, TGA, and DMTA. The degree of crystallinity of PBT was increased owing to the nucleation effects of OMMT. The addition of OMMT could assist in the char formation after thermal decomposition of PBT.

W. S. Chow would like to thank Toray Plastics (Malaysia) Berhad for kindly supplying the PBT resins.

References

1. Sinha Ray, S.; Okamoto, M. Prog Polym Sci 2003, 28, 1539.
2. Alexandre, M.; Dubois, P. Mater Sci Eng A 2000, 28, 1.
3. Zanetti, M.; Lomakin, S.; Camino, G. Macromol Mater Eng 2000, 279, 1.
4. Gallucci, R. R.; Patel, B. R. In Modern Polyesters: Chemistry and Technology of Polyesters and Copolyesters.; Scheirs, J.; Long, T. E., Eds.; Wiley: New York, 1973; p 293.
5. Chang, J. H.; An, Y. U.; Kim, S. J.; Im, S. S. Polymer 2003, 44, 5655.
6. Li, X. C.; Kang, T. Y.; Cho, W. J.; Lee, J. K.; Ha, C. S. Macromol Rapid Commun 2001, 22, 1306.
7. Xiao, J. F.; Hu, Y.; Wang, Z. Z.; Tang, Y.; Chen, Z. Y.; Fan, W. C. Eur Polym J 2005, 41, 1030.
8. Acierno, D.; Scarfato, P.; Amendola, E.; Nocerino, G.; Costa, G. Polym Eng Sci 2004, 44, 1012.
9. Chang, Y. W.; Kim, S. S.; Kyung, Y. B. Polym Int 2005, 54, 348.
10. Wu, D. F.; Zhou, C. X.; Fan, X.; Mao, D. L.; Bian, Z. Polym Degrad Stab 2005, 87, 511.
11. Shelley, J. S.; Mather, P. T.; De Vries, K. L. Polymer 2001, 42, 5849.
12. Scheirs, J. Compositional and Failure Analysis of Polymers: A Practical Approach; Wiley: New York, 2000.
13. Broza, G.; Kwiatkowska, M.; Roslaniec, Z.; Schulte, K. Polymer 2005, 46, 5860.
14. Mohd Ishak, Z. A.; Ariffin, A.; Senawi, R. Eur Polym J 2001, 37, 1635.
15. Wu, D.; Wu, L.; Zhang, M. Polym Degrad Stab 2006, 91, 1.